

## THE STABILITY OF LIZARDITE AND CHRYSOTILE

DAVID S. O'HANLEY

*Department of Mineralogy, Royal Ontario Museum, 100 Queen's Park, Toronto, Ontario M5S 2C6*

JOSEPH V. CHERNOSKY, JR.

*Department of Geology, University of Maine, Orono, Maine 04469, U.S.A.*

FREDERICK J. WICKS

*Department of Mineralogy, Royal Ontario Museum, 100 Queen's Park, Toronto, Ontario M5S 2C6*

### ABSTRACT

The method of dual networks was used to investigate phase relations in the MASH system amongst brucite (B), forsterite (F), aluminian lizardite (L), chrysotile (C), antigorite (A), talc (T), clinocllore (Cl), and water (W). Only nine of the 96 possible univariant equilibria, and two ([B,C] and [L,T,Cl]) of the 15 invariant points are calculated to be stable in the  $P(H_2O)$ - $T$  plane. The  $P(H_2O)$ - $T$  coordinates of invariant point [B,C] are determined by the intersection of the reactions  $L = F + T + Cl + W$  (1) and  $A = F + T + W$  (2). Reaction (1) shifts to lower temperatures and pressures with decreasing Al content of lizardite. Thus, invariant point [B,C], located at  $P(H_2O) > 25$  kbars for lizardite with high-Al content ( $> 9.0$  wt.%  $Al_2O_3$ ), shifts to  $P(H_2O) = 5$  kbars for lizardite with intermediate-Al content ( $\sim 3.5$  wt.%  $Al_2O_3$ ). As a result, the lizardite stability field decreases as the Al content of this phase decreases. Extrapolation of the above trend to lizardite with low-Al content ( $Al_2O_3 < 1.0$  wt.%) suggests that the topology of the phase diagram changes and conforms with that of the Al-free system. One result of this change is that the metastable reactions  $L = F + T + W$  and  $L + B = F + W$  are located at very low  $P(H_2O)$  for  $a(H_2O) = 1$ , suggesting that  $P(H_2O)$  may be an important independent variable in serpentinization. The phase diagram for low-Al lizardite is used to divide the  $P(H_2O)$  -  $T$  plane into regions characterized by the transition of one serpentine mineral to another. At  $P(H_2O)$  and  $T$  below invariant point [L, T] in the MSH system (the most common retrograde regime), forsterite reacts metastably to form lizardite as temperature decreases. At  $P(H_2O)$  and  $T$  above [L,T], forsterite reacts stably to form antigorite as temperature decreases or antigorite reacts to produce forsterite as temperature increases (the most common prograde regime). In chrysotile asbestos deposits, lizardite reacts metastably to form chrysotile as a matrix phase as  $P(H_2O)$  increases.

**Keywords:** lizardite, chrysotile, dual networks, serpentinization.

### SOMMAIRE

La méthode des réticules doubles a été utilisée pour étudier les équilibres dans le système MASH impliquant les phases brucite (B), forsterite (F), lizardite alumineuse (L), chrysotile (C), antigorite (A), talc (T), clinocllore (Cl) et

eau (E). Seulement neuf des 96 équilibres univariants possibles et deux ([B,C] et [L,T,Cl]) des 15 points invariants seraient stables dans le plan  $P(H_2O)$ - $T$ . Les coordonnées  $P$ - $T$  du point invariant [B,C] sont fixées par l'intersection des réactions  $L = F + T + Cl + E$  (1) et  $A = F + T + E$  (2). La courbe pour la première réaction est déplacée vers une température et une pression plus basses à mesure que la lizardite devient moins alumineuse. Le point invariant [B,C], situé à  $P(H_2O) > 25$  kbars pour une lizardite alumineuse (9.0% par poids de  $Al_2O_3$ ), serait donc déplacé à 5 kbars pour une lizardite à teneur intermédiaire en Al (3.5% de  $Al_2O_3$ ). Il en résulte que le champs de stabilité de la lizardite diminue avec sa teneur en Al. A la suite d'une extrapolation à une lizardite pauvre en Al ( $< 1.0\%$  de  $Al_2O_3$ ), nous préconisons un changement dans la topologie du diagramme des phases pour le rendre conforme au diagramme pour le système sans Al. Les réactions métastables  $L = F + T + E$  et  $L + B = F + E$  seraient situées à de très faibles valeurs de  $P(H_2O)$  pour  $a(H_2O) = 1$ , indications donc que la valeur de  $P(H_2O)$  ne serait pas une variable indépendante importante dans un milieu de serpentinisation. Le diagramme des phases pour la lizardite à faible teneur d'aluminium sert à diviser le plan  $P(H_2O)$  -  $T$  en régions de transition d'une forme de serpentine à une autre. A  $P(H_2O)$  et  $T$  inférieures au point [L, T] dans le système MSH (le milieu rétrograde le plus répandu), la forsterite réagit de façon métastable pour former de la lizardite à mesure que diminue la température. A  $P(H_2O)$  et  $T$  supérieures à [L,T], la forsterite réagit de façon stable pour former de l'antigorite à mesure que diminue la température, ou bien l'antigorite réagit pour produire de la forsterite avec une augmentation dans la température (le milieu prograde le plus important). Dans les gisements de chrysotile, la lizardite réagit de façon métastable pour former chrysotile dans la matrice avec une augmentation en  $P(H_2O)$ .

(Traduit par la Rédaction)

**Mots-clés:** lizardite, chrysotile, réticules doubles, serpentinisation.

### INTRODUCTION

The stability of lizardite with respect to chrysotile and antigorite has been of interest since lizardite was first recognized by Whittaker & Zussman (1956).

Deer *et al.* (1962) presented the first systematic evaluation of chrysotile, lizardite and antigorite, and their concluding statement has formed the basis for much of the research that followed: "If the three varieties have no essential chemical differences it could also be inferred that the formation of each polymorph in nature is favored by particular environmental conditions . . . It seems probable, however, that small chemical differences are associated with each of the three varieties."

This conundrum was partly solved, especially with regard to antigorite, as an understanding of the structures and crystal chemistry of the serpentine minerals developed. It was recognized that antigorite, which has a modulated structure (Guggenheim & Eggleton 1987), contains less Mg and OH than the ideal serpentine composition  $Mg_3Si_2O_5(OH)_4$  (Zussman 1954, Kunze 1961). In addition to the obvious difference between the planar structure of lizardite and the cylindrical structure of chrysotile, there is a fundamental difference in the stacking position of the successive layers in chrysotile compared to the stacking position in lizardite, and most other phyllosilicates (Wicks & O'Hanley 1988). Thus, lizardite and chrysotile are polymorphs, each with its own series of polytypes (Wicks & Whittaker 1975).

Results of wet-chemical and electron-microprobe analyses indicate that the ranges in chemical composition of lizardite and chrysotile are different, but that there is an overlap in composition at low Al and Fe contents (Whittaker & Wicks 1970, Dungan 1979, Wicks & Plant 1979). At increased Al contents the coupled substitution of Al for Si in the tetrahedral sheet, and of Al for Mg in the octahedral sheet, overcomes the misfit between the sheets, thus eliminating the possibility of the curved structures of chrysotile and antigorite and destroying the polymorphic relationship between lizardite and chrysotile. Substitution of Al in lizardite extends to amesite, in which  $\frac{1}{2}$  of the Mg and  $\frac{1}{2}$  of the Si are replaced by Al. The structure is planar through this composition range but adjusts in different ways at different compositions (Wicks & O'Hanley 1988).

The analytical results suggest that lizardite accepts slightly more Fe in substitution than antigorite, and considerably more than chrysotile (Wicks & Plant 1979). The structural differences between the polymorphs lizardite and chrysotile possibly lead to preferences for different cations if they are available, and thus to different but overlapping fields of stability (Caruso & Chernosky 1979). The  $P$ - $T$  coordinates of many reactions important to the serpentine system have been determined experimentally (Moody 1976, Evans *et al.* 1976, Caruso & Chernosky 1979), but little is known of the effects of minor components other than  $Fe^{2+}$  on the phase equilibria among the serpentine minerals. Serpentinites are dominated by Mg-rich minerals, so that

in most instances other cations, with the possible exceptions of Al, Cr, and  $Fe^{3+}$ , are present in such small amounts that their effect on serpentine equilibria is minimal (Evans 1977).

Petrographic observations indicate that lizardite, chrysotile and antigorite exhibit definite textural relationships to one another that transcend inferred age and origin of the serpentinization (Wicks & Zussman 1975, Wicks & Whittaker 1977, Wicks *et al.* 1977). Lizardite almost always forms pseudomorphic textures after olivine (Wicks & Whittaker 1977). In the infrequent occurrences of chrysotile in pseudomorphic textures, it is often intimately intermixed with lizardite (Cressey 1979). Prograde metamorphism produces antigorite with interpenetrating textures (Wicks & Whittaker 1977). Chrysotile asbestos deposits occur in serpentinites with a distinctive sequence of textures and mineralogy that can include all three serpentine minerals (Wicks & Whittaker 1977). One of the conclusions reached by Prichard (1979) in her study of samples from ophiolites and from the ocean floor was that lizardite formed from olivine and that chrysotile did not form until olivine had reacted out. Laurent & Hébert (1979) and Cogulu & Laurent (1984) also reached this conclusion for the serpentinites of southeastern Quebec. These petrographic observations suggest that equilibrium rather than kinetic factors affect the development of serpentine mineralogy. They also suggest that the relationship between lizardite and chrysotile transcends any particular bulk chemistry, which is the justification for the use of simplified chemographic models to analyze the serpentine system.

The relationship between lizardite and chrysotile can be explored fruitfully using chemographic analysis based on observations of natural occurrences and experimental data (Stout 1985, O'Hanley 1987a). Dual networks allow all three serpentine minerals to be included, together with other relevant phases in the chemography (O'Hanley 1987b).

Experimental data for the reaction aluminian (Al) lizardite = forsterite + talc + clinocllore + water, for two bulk compositions of lizardite, each with a different Al content (3.5 and 9 wt. %  $Al_2O_3$ ) suggest that the thermal stability of lizardite is greatly enhanced by the presence of Al (Caruso & Chernosky 1979). Frost (1975) found that lizardite (1-5 wt. %  $Al_2O_3$ ) persists beyond the serpentine-out reaction, antigorite (1-3 wt. %  $Al_2O_3$ ) = forsterite + talc + chlorite + water. The experimental work of Chernosky (1975) and Caruso & Chernosky (1979) and the observations and microprobe data of Frost (1975) indicate that substitution of Al in lizardite increases its thermal stability.

In the present paper, the approach used by O'Hanley (1987b) is extended to the MASH system containing the phases brucite, forsterite, chrysotile,

antigorite, talc, aluminian lizardite, clinochlore, and water. This method investigates the  $P$ - $T$  relationships among minerals of fixed composition. To remove the chemographic degeneracy between lizardite and chrysotile, we have assumed that Al partitions into lizardite rather than chrysotile. This assumption is not strictly correct because available microprobe data suggest that lizardite and chrysotile with identical but low Al contents commonly coexist (Wicks & Plant 1979).

#### METHODOLOGY AND CHEMOGRAPHY

The relevant phases in the MASH system are shown in Figure 1, projected through water. Details of the method used to investigate this system are given in Stout (1985) and O'Hanley (1987a). In the method, an  $n$ -component,  $(n+3)$ -phase system is defined, and the unique divariant fields are assembled to form a dual network. Inversion of the dual network yields a basic form that includes all of the

stable equilibria; the addition of metastable equilibria to the basic form yields a potential solution. For a given chemography of  $n$ -component  $(n+3)$ -phases, all potential solutions are generated. This set of potential solutions is explored to find the one most consistent with available geological and thermochemical data.

The phases selected for chemographic analysis are those observed in serpentinites: brucite, forsterite, lizardite (with a specific Al content), chrysotile (Al-free), antigorite, talc, clinochlore and water. Clinochlore was included because 1) it has been observed in mesh textures (Cressey 1979), 2) it often is the Al-bearing phase associated with lizardite and chrysotile (Evans 1977), and 3) its role in serpentinization has not been fully assessed.

Talc was initially omitted to obtain a  $(n+3)$ -phase system because the assemblage antigorite + chlorite is considered to be more stable than lizardite + talc (Springer 1974, Pinsent & Hirst 1977). Thus all of the invariant points in the  $(n+3)$ -phase system are

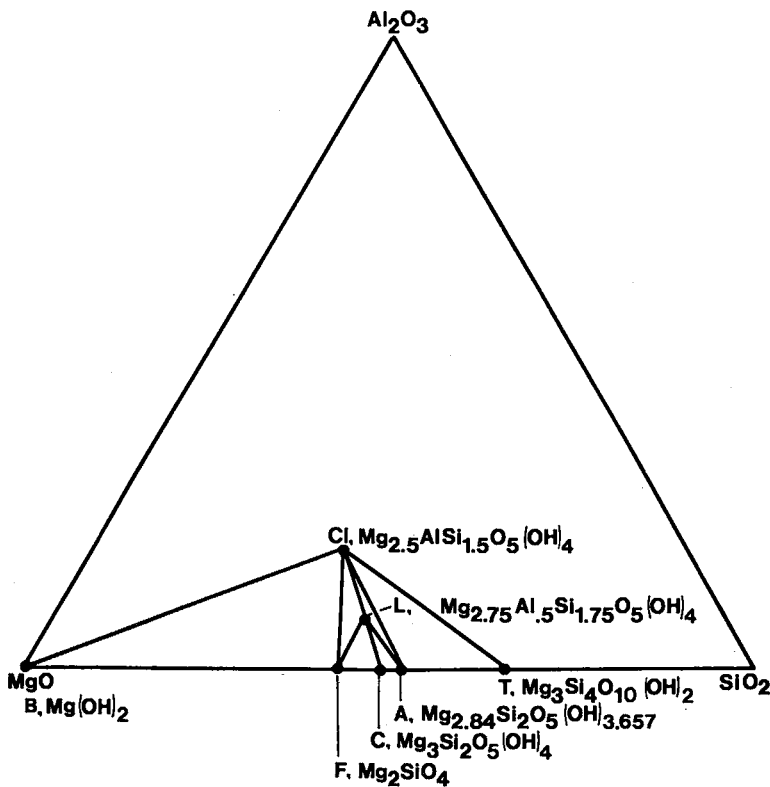


FIG. 1. Chemography for the MASH system, involving the phases brucite (B), forsterite (F), aluminum-free chrysotile (C), antigorite (A), talc (T), aluminian lizardite (L), and clinochlore (Cl), projected through water (W). Solubility of Al in lizardite rather than in chrysotile removes the polymorphic degeneracy between lizardite and chrysotile.

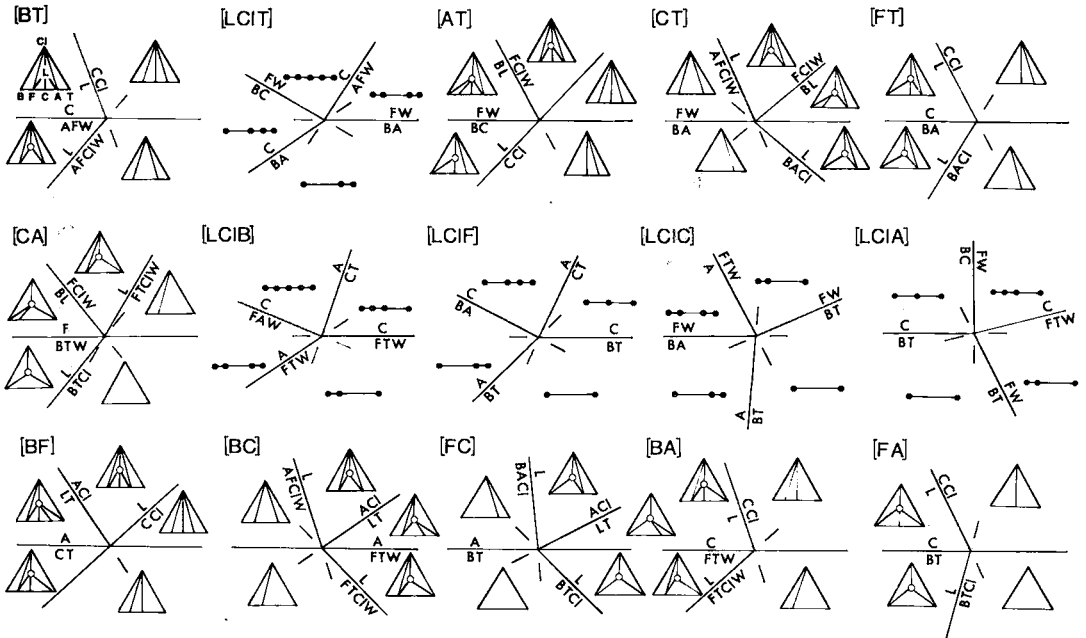


FIG. 2. Invariant point maps for the MASH system, involving the phases brucite, forsterite, aluminum-free chrysotile, antigorite, talc, aluminian lizardite, and clinocllore, projected through water. The top row of invariant points belongs to the talc-absent, six-phase system. The bottom two rows of invariant points include talc as an additional phase. Note that divariant fields used in invariant point maps include assemblages not affected by reactions at the invariant point. Symbols are defined in Figure 1.

talc-absent invariant points and they are labeled as such in the first row of Figure 2. As there are only two Al-bearing phases, both must be present in or absent from a given reaction. The result is that invariant points [L] and [Cl] coincide and are labeled [L,Cl]. The five invariant points for the  $n+3$  system can be assembled into 20 potential solutions.

#### ELIMINATION OF POTENTIAL SOLUTIONS

The phase diagrams shown in Figures 3, 4, and 8 were calculated using the program GEOCALC (Berman *et al.* 1986) and the thermodynamic data of Berman (1988) for all phases except lizardite. Thermodynamic data for the lizardite crystalline solutions L(0.2) and L(0.5), where the number in parentheses is given by  $x$  in the formula  $(Mg_{6-x}Al_x)(Si_{4-x}Al_xO)_{10}(OH)_8$ , are from Chernosky *et al.* (1988). Molar volumes for L(0), L(0.2), and L(0.5) were taken from Chernosky (1975) and Caruso & Chernosky (1979). All thermodynamic properties are consistent with Berman's (1988) thermodynamic data-base. The absence of phase-equilibrium data for L(0) precludes calculation of L(0)-bearing equilibria.

The stable equilibria involving L(0.5) and L(0.2)

are shown in Figures 3 and 4, respectively. The metastable reactions chrysotile = forsterite + antigorite + water, and lizardite = chrysotile + clinocllore, which were calculated using the same data-base, are plotted also. These calculations suggest that the talc-absent invariant points [C,T] and [L,T,Cl] are stable. This conclusion eliminates potential solutions 1-4, 7-18 and 20, in which one or both of these invariant points are metastable. The remaining solutions are 5, 6 and 19 (Fig. 5). The negative slope of the stable reaction chrysotile = brucite + antigorite (Fig. 3 or 4) and the positive slope of the metastable reaction lizardite = chrysotile + clinocllore (Fig. 3 or 4) suggest that invariant point [F,T] is metastable and located at low pressure. The positive slope of the reaction chrysotile = forsterite + antigorite + water at low pressure and the steep slope of reaction lizardite = chrysotile + clinocllore suggest that invariant point [B,T] is metastable and located at high pressure. These observations eliminate solutions 6 and 19, leaving 5. Talc was then added to the chemography, yielding a 3-component, 7-phase system. The additional invariant points for the augmented system are shown in the lower two rows of Figure 2. A portion of the resulting phase diagram is shown in Figure 6.

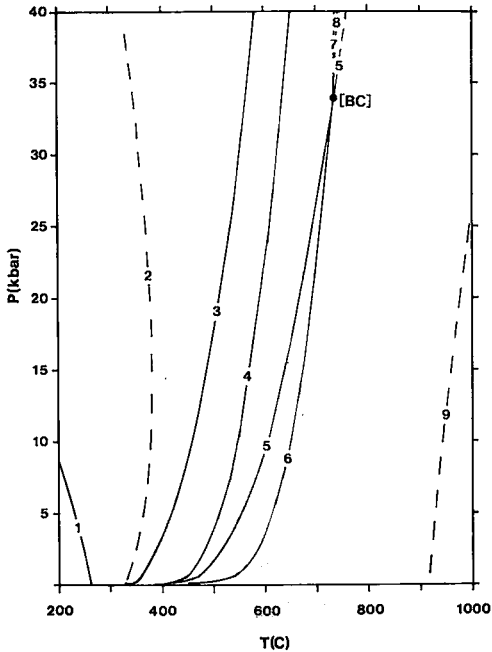


FIG. 3. Calculated reactions for the model containing L(0.5) to 40 kbars and 1000°C. Solid and dashed lines represent stable and metastable reactions, respectively. Dashed line is the critical curve for water. Numbered reactions are (symbols defined in caption to Figure 1): 1.  $C = B + A$ ; 2.  $C = F + A + W$ ; 3.  $B + A = F + W$ ; 4.  $B + L = F + Cl + W$ ; 5.  $A = F + T + W$ ; 6.  $L = F + T + Cl + W$ ; 7.  $L + T = A + Cl$ ; 8.  $L = F + A + Cl + W$ ; 9.  $L = C + Cl$ . See text for discussion.

#### DISCUSSION

The phase diagram shown in Figure 6 is similar to that proposed by Caruso & Chernosky (1979) because both diagrams contain [C,T] and [B,C] stable. O'Hanley (1987b) presented a phase diagram for the MSH system containing brucite, forsterite, lizardite, chrysotile, antigorite, talc and water in which lizardite and chrysotile are treated as polymorphs (Fig. 7).

Figures 6 and 7 illustrate the topological relationships among several invariant points pertinent to the stability of lizardite and chrysotile. These diagrams are oriented in the  $P(H_2O)$ - $T$  plane, but no  $P(H_2O)$ - $T$  coordinates are shown. Figures 3 and 4 do show  $P(H_2O)$ - $T$  coordinates and therefore exhibit the geometrical relationships among the invariant points for L(0.5) and L(0.2), respectively.

Comparison of Figures 3 and 4 with Figure 6 indicates that several invariant points shown in Figure 6 are not in an accessible region of the  $P(H_2O)$ - $T$

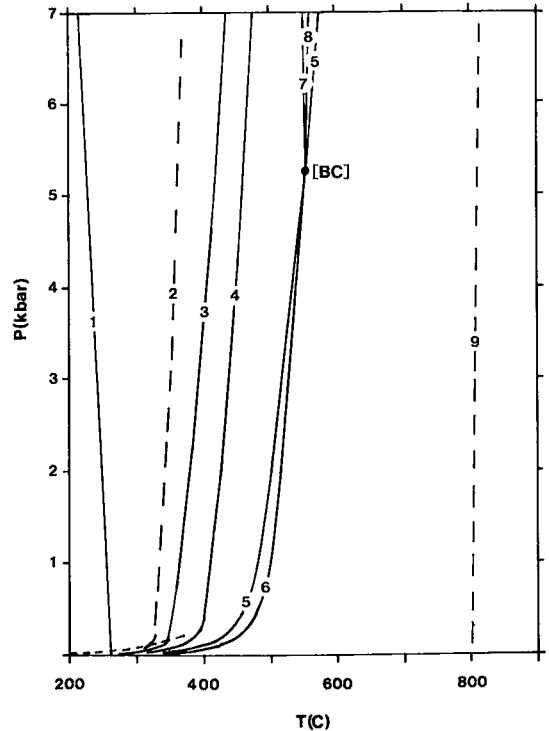


FIG. 4. Calculated reactions for the model containing L(0.2) to 7 kbars and 900°C. Solid and dashed lines represent stable and metastable reactions, respectively. Dashed line is the critical curve for water. See caption of Figure 3 for key to numbered reactions. See text for discussion.

plane with respect to serpentinization. The thermodynamic data of Berman (1988) for the MSH system do not permit the reaction chrysotile + talc = antigorite to occur at a  $T$  greater than 25°C, which implies that invariant points [B,L] and [B,F] do not occur above 25°C. This finding suggests that the pressure axis is located somewhere between invariant points [B,L,Cl] and [L,T,Cl], which places invariant point [B,L,Cl] into an inaccessible region of the  $P(H_2O)$ - $T$  plane. The steep slopes of reactions chrysotile = brucite + antigorite and lizardite = chrysotile + clinocllore indicate that invariant points [F,T] and [B,F] are located at a negative pressure, so that the temperature axis is located somewhere between invariant points [B,C] and [F,T]. This situation leaves only invariant points [L,T,Cl] and [B,C] in an accessible region of the  $P(H_2O)$ - $T$  plane, with invariant point [C,T] at a  $P$  above 25 kbars for L(0.2). Similar arguments using the calculations of Berman *et al.* (1986) for the MSH system in Figure 7 indicate that only invariant points

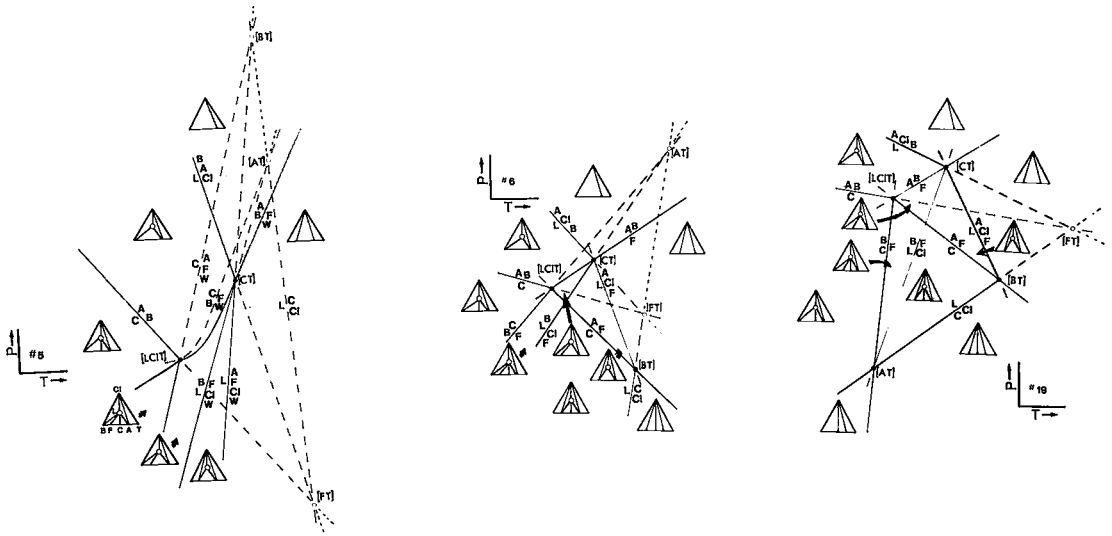


FIG. 5. Oriented potential solutions 5,6 and 19 for the 7-phase MASH system, involving brucite, forsterite, aluminum free chrysotile, antigorite, aluminian lizardite, and clinocllore, projected through water. Solid lines represent stable reactions, long-dash lines represent metastable reactions, and short-dash lines represent doubly metastable reactions. The differences among the solutions involve the stability of invariant points [A,T], [B,T], and [F,T].

[L,T], [C,T] and [F,T] are in an accessible region of the  $P(\text{H}_2\text{O})$ - $T$  plane.

Comparison of the two phase diagrams (Figs. 6, 7) indicates that each serpentine mineral occupies a specific region of  $P$ - $T$  space. At present, none of the reactions involving more than one serpentine mineral has been calibrated experimentally. Minor elements will affect the extent of the overlap in stability; for instance, lizardite and chrysotile overlap in stability in Figure 6 because of variable Al content but occupy distinct regions of  $P$ - $T$  space in Figure 7. In general terms, antigorite is the high-temperature serpentine mineral, whereas lizardite and chrysotile are the low-temperature serpentine minerals. In the MSH system, chrysotile is the low-pressure, low-temperature serpentine mineral, whereas lizardite is the high-pressure, low-temperature serpentine mineral.

Further comparison of the two phase diagrams must take into account the different topologies. One topology can be derived from the other. Starting with the diagram for high-Al lizardite (Fig. 6), the lizardite-bearing reactions shift to lower temperature as the Al content of lizardite is reduced. The invariant points must shift to lower temperatures as well. For example, invariant point [B,C] shifts to lower temperature along the reaction antigorite = forsterite + talc + water as the reaction  $L_{ss} = \text{forsterite} + \text{talc} + \text{clinocllore} + \text{water}$  shifts to lower temperatures. Once the Al content of lizardite reaches some low concentration, invariant point [B,C] passes over invariant point [B,L], rendering [B,C] metastable (Fig. 7).

We have divided lizardite compositions into three groups on the basis of Al content. High-Al lizardite contains more than 3.5 wt.%  $\text{Al}_2\text{O}_3$ . Two reactions involving high-Al lizardite have been reversed experimentally and are described by Figure 6. Low-Al lizardite contains less than 1 wt.%  $\text{Al}_2\text{O}_3$  and can be considered a polymorph of chrysotile (Wicks & Plant 1979). Reactions involving low-Al lizardite are described by Figure 7. Intermediate-Al lizardite comprises the remaining group. This type of lizardite is found in orthopyroxene bastite (Wicks & Plant 1979, Dungan 1979), but this material has not been studied in detail.

Further comparison of the two diagrams shows clearly that the extent of the stability field for lizardite depends on composition. For example, in Figure 6 invariant points [B,L,Cl] and [L,T,Cl] are metastable, whereas [B,L] and [L,T] are stable in Figure 7. The thermal stability of lizardite decreases with decreasing Al content. Although experimental work is restricted to high-Al lizardite, the calibrations place useful constraints on the phase relations of intermediate- and low-Al varieties of lizardite and are therefore useful for interpretations of the assemblages found in serpentinites.

#### Importance of water pressure

Sanford (1981) discussed the role of water pressure  $P(\text{H}_2\text{O})$  as an independent variable during retrograde and prograde serpentinization. Bruton & Helgeson (1983) discussed the effects of  $P(\text{H}_2\text{O}) <$





### Chemographic models and the serpentinization of olivine

Wicks & Whittaker (1977) proposed a model to account for the observed mineralogy and texture of serpentinites. The parameters used were temperature and the presence or absence of antigorite and penetrative deformation. Various combinations of these parameters yielded 8 regimes of serpentinization (Table 1).

The refined model presented here relates the regimes of Wicks & Whittaker (1977) to the serpentine phase diagram (Fig. 7) of O'Hanley (1987b) (Table 1). Unfortunately, the lack of an adequate solution-model for lizardite crystalline solutions precludes the thermodynamic calculation of the lizardite-bearing reactions depicted on Figure 7 in the  $P(\text{H}_2\text{O})$ - $T$  plane. The 8 regimes of Wicks & Whittaker (1977) reduce to 4 for the following reasons. Firstly, although penetrative deformation influences texture, the deviatoric stress does not seem to exert a great influence on mineralogy and does not need to be considered. Secondly, the presence of antigorite reflects a change in intensive variables rather than sluggish reaction-kinetics. Thus, paths through the  $P(\text{H}_2\text{O})$ - $T$  plane represented by transitions among serpentine minerals depend solely on  $T$  and  $P(\text{H}_2\text{O})$ . The regimes of serpentinization referred to above are redefined in the right-hand column of Table 1 and are referred to by letters.

Regime A, serpentinization with decreasing temperature, occurs at temperatures and pressures above invariant point [L, T]. This type of serpentinization, during which the hydration of olivine produces antigorite, is not common, although it has been reported in the Glen Urquhart serpentinite (Wicks 1984) and the Trinity peridotite (Peacock 1987), and has been inferred for the Fox River Sill (Wicks & Whittaker 1977).

The more frequently encountered retrograde regime B is located at temperatures and water pressures below invariant point [L, T]. The metastable reaction forsterite + water = brucite + lizardite is operative, and pseudomorphic textures are produced. This regime is promoted either by serpentinization initiated by a free fluid phase, such as a large quantity of meteoric water, or by a low  $\alpha(\text{H}_2\text{O})$  due to intergranular water.

The prograde regime C occurs where serpentinization is complete, and water pressure and perhaps temperature increase, such that lizardite reacts to produce chrysotile as a matrix phase. This regime is characteristic of chrysotile asbestos deposits (Wicks & Whittaker 1977).

The prograde sequence more frequently encountered, represented by regime D, occurs above invariant point [L, T]. Lizardite or chrysotile (or both) react to produce antigorite, which reacts to produce

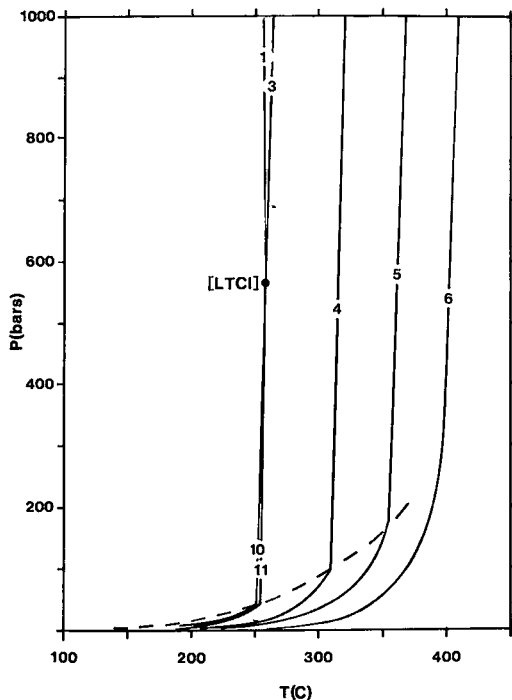


Fig. 8. Calculated reactions for the model involving L(0.2) for  $\alpha(\text{H}_2\text{O}) = 0.3$  from 1 to 1000 bars. To be compared with Figure 4. Numbered reactions in addition to those in Figure 4 are: 10.  $B + C = F + W$ ; 11.  $C = F + A + W$ . See text for discussion.

TABLE 1. CLASSIFICATIONS OF SERPENTINIZATION

| Type | T    | Wicks and Whittaker* (1977)<br>Antigorite | Foliation | New Designation<br>Regime | Location in<br>P-T Space                   |
|------|------|---|-----------|---------------------------|--|
| 1.   | down | yes<br>pseudomorphic**                    | no        | A                         | above [BC] or [BL]                         |
| 2.   | down | yes                                       | yes       |                           |  |
| 3.   | down | no<br>pseudomorphic                       | no        | B                         | below [BC] or [BL]                         |
| 4.   | down | no  | yes       |                           |  |
| 5.   | up   | no<br>transitional                        | no        | C                         | T below [BC] or [BL]<br>P below [BF], [FT] |
| 6.   | up   | no  | yes       |                           |  |
| 7.   | up   | yes                                       | no        | D                         | above [BC] or [BL]                         |
| 8.   | up   | yes                                       | yes       |                           |  |

\*T: Temperature increasing (up) or decreasing (down); Antigorite: nucleation (yes) or absence (no); Foliation: presence (yes) or absence (no) of shearing.

\*\* Regimes that produce pseudomorphic textures are labeled, Regime 5 produces the transitional texture.

forsterite with increasing temperature.

### CONCLUSIONS

The chemographic models presented here incorporate and exploit fully the available experimental data and petrological observations. However, the lack of a solution model for lizardite restricts the use of Figure 7.

The conclusions that the stability of lizardite is a function of its Al content and that its occurrence after olivine represents a metastable reaction at either low  $a(\text{H}_2\text{O})$  or low  $P(\text{H}_2\text{O})$  yield insight into the serpentinization process and the development of serpentine textures and, in particular, into the role of  $P(\text{H}_2\text{O})$  and  $a(\text{H}_2\text{O})$ . Figures 3 and 4 give an indication of the temperatures and pressures associated with the different regimes of serpentinization.

### ACKNOWLEDGEMENTS

The authors thank Ron Frost for his comments on serpentine equilibria and on the role of water activity. We also thank the photography department at the Royal Ontario Museum for providing prints of the figures.

### REFERENCES

- BERMAN, R.G. (1988): Internally consistent thermodynamic data for minerals in the system  $\text{Na}_2\text{O}-\text{K}_2\text{O}-\text{CaO}-\text{MgO}-\text{FeO}-\text{Fe}_2\text{O}_3-\text{Al}_2\text{O}_3-\text{SiO}_2-\text{TiO}_2-\text{H}_2\text{O}-\text{CO}_2$ . *J. Petrol.* **29**, 445-522.
- , ENGI, M., GREENWOOD, H.J. & BROWN, T.H. (1986): Derivation of internally consistent thermodynamic data by the technique of mathematical programming: a review with application to the system  $\text{MgO}-\text{SiO}_2-\text{H}_2\text{O}$ . *J. Petrol.* **27**, 1331-1364.
- BRUTON, C.J. & HELGESON, H.C. (1983): Calculation of the chemical and thermodynamic consequences of differences between fluid and geostatic pressure in hydrothermal systems. *Am. J. Sci.* **283-A**, 540-588.
- CARUSO, L.J. & CHERNOSKY, J.V., JR. (1979): The stability of lizardite. *Can. Mineral.* **17**, 757-769.
- CHERNOSKY, J.V., JR. (1975): Aggregate refractive indices and unit-cell parameters of synthetic serpentine in the system  $\text{MgO}-\text{Al}_2\text{O}_3-\text{SiO}_2-\text{H}_2\text{O}$ . *Am. Mineral.* **60**, 200-208.
- , BERMAN, R.G. & BRYNDZIA, L.T. (1988): Serpentine and chlorite equilibria. In *Hydrous Phyllosilicates other than Micas* (S.W. Bailey, ed.). *Mineral. Soc. Am., Rev. Mineral.* **19**, 295-346.
- COGULU, E. & LAURENT, R. (1984): Mineralogical and chemical variations in chrysotile veins and peridotite host-rocks from the asbestos belt of southern Quebec. *Can. Mineral.* **22**, 173-183.
- CRESSEY, B.A. (1979): Electron microscopy of serpentine textures. *Can. Mineral.* **17**, 741-756.
- DEER, W.A., HOWIE, R.A. & ZUSSMAN, J. (1962): *Rock-Forming Minerals. III. Sheet Silicates*. Longman, Green and Co., London.
- DUNGAN, M.A. (1979): A microprobe study of antigorite and some serpentine pseudomorphs. *Can. Mineral.* **17**, 771-784.
- EVANS, B.W. (1977): Metamorphism of alpine peridotites and serpentinites. *Annu. Rev. Earth Planet Sci.* **5**, 397-448.
- , JOHANNES, W., OTTERDOOM, H. & TROMMSDORFF, V. (1976): Stability of chrysotile and antigorite in the serpentine multisystem. *Schweiz. Mineral. Petrogr. Mitt.* **56**, 79-93.
- FROST, B.R. (1975): Contact metamorphism of serpentine, chloritic blackwall and rodingite at Paddy-Go-Easy Pass, Central Cascades, Washington. *J. Petrol.* **16**, 272-313.
- (1985): On the stability of sulfides, oxides, and native metals in serpentine. *J. Petrol.* **26**, 31-63.
- GUGGENHEIM, S. & EGGLETON, R.A. (1987): Modulated 2:1 layer silicates: review, systematics and predictions. *Am. Mineral.* **72**, 724-738.
- KUNZE, G. (1961): Antigorit strukturtheoretische Grundlagen und ihre praktische Bedeutung für die weitere Serpentin-forschung. *Fortschr. Mineral.* **39**, 206-324.
- LAURENT, R. & HÉBERT, Y. (1979): Paragenesis of serpentine assemblages in harzburgite tectonite and dunite cumulate from the Quebec Appalachians. *Can. Mineral.* **17**, 857-869.
- MOHR, R.E. & STOUT, J.H. (1980): Multisystems nets for systems of  $n + 3$  phases. *Am. J. Sci.* **280**, 143-172.
- MOODY, J.B. (1976): An experimental study on the serpentinization of iron-bearing olivines. *Can. Mineral.* **14**, 462-478.
- O'HANLEY, D.S. (1987a): The construction of phase diagrams by means of dual networks. *Can. Mineral.* **25**, 105-119.
- (1987b): A chemographic analysis of magnesian serpentinites using dual networks. *Can. Mineral.* **25**, 121-133.
- PEACOCK, S. (1987): Serpentinization and infiltration metasomatism in the Trinity peridotite, Klamath province, northern California: implications for subduction zones. *Contrib. Mineral. Petrol.* **95**, 55-70.
- PINSENT, R.H. & HIRST, D.M. (1977): The metamorphism of the Blue River ultramafic body, Cassiar, British Columbia, Canada. *J. Petrol.* **18**, 567-594.

- PRICHARD, H.M. (1979): A petrographic study of the process of serpentinisation in ophiolites and the ocean crust. *Contrib. Mineral. Petrol.* **68**, 231-241.
- SANFORD, R.F. (1981): Mineralogical and chemical effects of hydration reactions and applications to serpentinization. *Am. Mineral.* **66**, 290-297.
- SPRINGER, R.K. (1974): Contact metamorphosed ultramafic rocks in the western Sierra Nevada foothills. *J. Petrol.* **15**, 160-195.
- STOUT, J.H. (1985): A general chemographic approach to the construction of ternary phase diagrams, with applications to the system  $\text{Al}_2\text{O}_3\text{-SiO}_2\text{-H}_2\text{O}$ . *Am. J. Sci.* **285**, 385-408.
- WENNER, D.B. & TAYLOR, H.P., JR. (1971): Temperatures of serpentinization of ultramafic rocks based on  $\text{O}^{18}/\text{O}^{16}$  fractionation between coexisting serpentine and magnetite. *Contrib. Mineral. Petrol.* **32**, 165-185.
- WHITTAKER, E.J.W. & WICKS, F.J. (1970): Chemical differences among the serpentine "polymorphs": a discussion. *Am. Mineral.* **55**, 1025-1047.
- \_\_\_\_\_ & ZUSSMAN, J. (1956): The characterization of serpentine minerals by X-ray diffraction. *Mineral. Mag.* **31**, 107-126.
- WICKS, F.J. (1984): Deformation histories as recorded by serpentinites. I. Deformation prior to serpentinization. *Can. Mineral.* **22**, 185-195.
- \_\_\_\_\_ & O'HANLEY, D.S. (1988): Serpentine minerals: structures and petrology. In *Hydrous Phyllosilicates other than Micas* (S.W. Bailey, ed.). *Mineral. Soc. Am., Rev. Mineral.* **19**, 91-168.
- \_\_\_\_\_ & PLANT, A.G. (1979): Electron microprobe and X-ray microbeam studies of serpentine textures. *Can. Mineral.* **17**, 785-830.
- \_\_\_\_\_ & WHITTAKER, E.J.W. (1975): A reappraisal of the structures of the serpentine minerals. *Can. Mineral.* **13**, 227-243.
- \_\_\_\_\_ & \_\_\_\_\_ (1977): Serpentine textures and serpentinization. *Can. Mineral.* **15**, 459-488.
- \_\_\_\_\_, \_\_\_\_\_ & ZUSSMAN, J. (1977): An idealized model for serpentine textures after olivine. *Can. Mineral.* **15**, 446-458.
- \_\_\_\_\_ & ZUSSMAN, J. (1975): Microbeam X-ray diffraction patterns of the serpentine minerals. *Can. Mineral.* **13**, 244-258.
- ZUSSMAN, J. (1954): Investigation of the crystal structure of antigorite. *Mineral. Mag.* **30**, 498-512.

*Received February 12, 1988, revised manuscript accepted November 14, 1988.*